# City Research Online

## City, University of London Institutional Repository

# Risk management of climate impact for tourism operators: An empirical analysis on ski resorts

Laura Ballotta[a], Gianluca Fusai[a,b], Ioannis Kyriakou[a,*], Nikos C. Papapostolou[a], Panos K. Pouliasis[a]

[a]*Cass Business School, City, University of London, 106 Bunhill Row, London EC1Y 8TZ, UK*
[b]*Dipartimento di Studi per l'Economia e l'Impresa, Università del Piemonte Orientale, Via Perrone 18, 28100 Novara, Italy*

## Abstract

The aim of this paper is to analyze the performance of hedging strategies based on snow and temperature options developed by ski operators to protect their profitability under adverse changes in climatic conditions. The setup is based on a joint non-parametric model for snow and temperature aimed at providing a modelling support for the assessment of the impact of these weather variables on the number of visitors at the ski resort. The analysis is carried out considering the case of Austrian Alps, and examines: i) the ability of the proposed approach to provide a realistic representation of the true data-generating process; ii) the variability reduction in the Profit and Loss of the ski operator offered by the suggested strategies; and iii) the tradeoff between the budget earmarked for hedging and profitability protection.

*Keywords:* Ski tourism; Climate change; Weather variables; Block bootstrap; Risk management; Options; Profitability

## 1. Introduction

The tourism sector plays an important role in many economies; for example, in Europe, its total contribution (direct, indirect and induced) to EU GDP and overall EU employment is, respectively, 10.2% and 11.6% (WTTC 2017). In particular, winter tourism's economic impact varies across different regions and areas, but for some of these, such as the Alpine region, it represents one of the main sources of income for local population across several industries, including accommodation, food services, transportation, arts and entertainment, and retail trade. In Austria and Switzerland, for example, the winter tourism industry is estimated to account for up to 49% of the countries' annual overnight stays (ANTO 2016, STV-FST 2016), to which a multiplier effect applies to account for income employment, government revenues and other inter-industrial relations. The tourism sector, though, is one of the most weather-sensitive ones, and winter tourism, in particular, is highly dependent on the level and reliability of the snow cover; as such, it has been earmarked as one of the most vulnerable industries to climate change (see Dawson and Scott 2013, for example).

---

*Correspondence
  *Email addresses:* `l.ballotta@city.ac.uk` (Laura Ballotta), `gianluca.fusai.1@city.ac.uk` & `gianluca.fusai@uniupo.it` (Gianluca Fusai), `ioannis.kyriakou@city.ac.uk` (Ioannis Kyriakou), `n.papapostolou@city.ac.uk` (Nikos C. Papapostolou), `p_pouliasis@city.ac.uk` (Panos K. Pouliasis)

Climate change is one of the most pressing global challenges society faces today. The United Nations has highlighted the potential for climate change to cause major disruption to national economies (see `https://www.un.org/sustainabledevelopment/climate-change-2/`), also due – amongst others – to negative impacts on agriculture and tourism. Given the high degree of adaptive capacity and flexibility of tourists, entire tourism sectors may lose attractiveness due to climate change. For instance, a study by Cavallaro et al. (2017) for South Tyrol puts in evidence a forecast shift in tourism expenditure from the winter to the summer season, as Alpine regions gain attractiveness in summer due to more temperate conditions compared to hotter Mediterranean regions, whilst they lose it in winter due to less reliable natural snow cover. Further evidence of the impact of climate change on the ski tourism segment is offered, for example, in Wolfsegger et al. (2008) and Wyss et al. (2014).

Adaptation strategies aimed at supporting ski tourism operators in managing the impact of weather variability and climate change are evolving along three main directions (see Scott and McBoyle 2006, Bank and Wiesner 2011). These include protection of the affected businesses in the form of snowmaking, slope contouring, landscaping and glacier protection; revenue diversification beyond traditional ski activities which, in many instances, leads to all-season facilities; and sharing of risks of financial impacts by either adopting a conglomerate business model or accessing the financial market for products such as weather derivatives.

Although snowmaking is the most common adaptation strategy, Scott and McBoyle (2006) highlight how this raises important questions about its sustainability in certain locations, its environmental impact, and consequent potential government restrictions on, for example, the use of additives to help artificial snow last longer in above-average temperature conditions (like in Austria, for example, see Wolfsegger et al. 2008) and on water access rights in certain regions. Further, snowmaking and other technical strategies as well as strategies based on revenue diversification do involve high investment costs for infrastructure and operating costs, especially in higher-average temperature conditions (see, for example, Damm et al. 2014 for a cost-revenue study of snowmaking related to a site in Austria).

In this context, weather derivatives can represent a useful complementary measure to the other adaptation strategies for hedging against weather variability and climate change risk (see, for example, Damm et al. 2014, Damm et al. 2017, Dawson and Scott 2013, Toeglhofer et al. 2012, and references therein). Indeed, this class of products can play a significant role not only in hedging against non-catastrophic weather risk, but also in supporting other adaptation strategies as they can offer flexible means for stabilizing business profitability year-on-year and developing a suitable investment planning. In fact, they provide protection against lower-risk higher-probability scenarios, and are characterized by a payout which is usually based on a weather index (such as temperature level, snow level and rainfall); this latter feature guarantees at the same time transparency and promptness in the settlements, as these are irrespective of the actual impact of weather on companies. These features are in sharp contrast with conventional weather insurance, which instead is focused on higher-risk lower-probability events (one-time catastrophe, natural disaster) and are characterized by payouts based on a demonstrated loss. Transparency and settlements' promptness of weather derivatives might also justify the interest and attention they attract from ski operators (Bank and Wiesner 2011);

although their applicability is hindered by a number of factors such as product and practice knowledge, access to the necessary financial resources, related high fixed costs, counterparty risk due to the over-the-counter nature of these contracts, transparency and basis risk.

In this paper, we focus our attention on ski tourism, the core of winter tourism, with the goal of proposing possible risk management strategies based on weather derivatives, such as snow and temperature options, which are relatively transparent, easy to use and maintain, and can help protect the profitability of ski resorts. Due to the close links between these operators and their local communities, reducing the resort exposure to weather-induced risk also contributes to stabilizing the economies of such communities and protecting their investments.

In details, we propose a joint non-parametric model for snow and temperature aimed at capturing the impact of these weather variables on ski operation viability and visitors' decisions, and consequently the number of visitors at a given ski resort. This latter component becomes the main reference variable for the estimation of the ski resort revenues in need of protection. Specifically, we identify snow depth as a key variable (see Falk and Hagsten 2016, and references therein) as, in order to determine the economic viability of ski areas, operators in Europe and North America use the so-called 100-day rule, according to which a snow depth of at least 30cm is required for at least 100 days per season (see, for example, Abegg et al. 2007, Steiger and Abegg 2013).

Our choice for a non-parametric model is in contrast with previous literature, such as Beyazit and Koc (2010) who impose a normal distribution to the (cumulative) level of the snow. A non-parametric approach constrains the shape of the fitted distribution of interest to a much lesser degree than parametric methods. The proposed methodological framework: i) is parsimonious and simple, requiring the estimation of only a few parameters, and the use of only standard statistical methods; ii) can flexibly capture dynamics that may contain trend and seasonality; iii) is extensible, i.e., may readily be modified to accommodate additional features, if desired, or weather variables such as rainfall, wind speed and global radiation; iv) is inexpensive in the sense that its implementation and analysis requires only standard, easily accessible software and data, as well as minimal human maintenance and oversight; v) does not impose a restriction of convenience on the distribution of the snow level; and vi) has very good statistical properties if a large dataset is available, such as for snow and temperature that exceeds 55 years.

The hedging strategies proposed in this paper consider different portfolios of options on snow and temperature, with the aim of stabilizing ski resort revenues. As these are significantly affected by visitors' decisions, which in turn are conditioned by a number of variables in addition to snow cover and temperature, such as available holidays, transportation and country of origin, there is an inevitable intrinsic basis risk in the hedge (technological basis risk). Additional basis risk arising with weather derivatives is the so-called spatial basis risk due to difference between the reference weather index the derivative contract is linked to and the actual weather experienced at the location of interest. Thus, following standard financial theory for dealing with basis risk, our construction relies on the minimum variance principle applied to the position as a whole, after the cost of implementation is accounted for. The alternative strategies are then tested in terms of hedging effectiveness, tradeoff with the actual cost, and robustness with respect to spatial basis risk.

We note that we focus on options as our derivative contracts of choice; this is motivated by the results of Broll et al. (2001) and Manfredo and Richards (2009), which suggest that the convexity of options makes them more appealing for hedging than forwards and other linear derivatives in the presence of non-linear risk exposure. Indeed, the work of Damm et al. (2014) highlights the high non-linearity between the level of snow and the number of visitors at the ski resorts, and therefore the revenues exposed to risk. The importance of non-linear models and methods in tourism demand is also highlighted in Baggio and Sainaghi (2016). Beyazit and Koc (2010) adopt snow options as well for hedging in their study, although the issue of basis risk is not dealt with; Đorđević (2018) and Tang and Jang (2011, 2012), on the other hand, consider the case of snowfall forwards in the context of the minimum variance principle.

The paper is organized as follows. In Section 2, we introduce the dataset of interest; in Section 3, we illustrate the proposed modelling and methodological framework and perform empirical model comparisons. In Section 4, we present a preliminary empirical analysis which leads to the construction, implementation and testing of the proposed hedging strategies, discussed in Section 5. Finally, Section 6 offers concluding remarks and highlights some pressing directions for future research.

## 2. Data

The dataset we consider includes observations of both snow and temperature levels. A systematic climate change detection and analysis of sub-monthly climate extremes requires dataset with daily resolution. For this purpose, we use daily observational climatic time series that have been compiled for the European Climate Assessment (ECA) available from `http://www.ecad.eu/` (Klein Tank et al. 2002). The European Climate Assessment and Dataset (ECA&D) is a database of daily meteorological station observations across Europe and is gradually being extended to countries in the Middle East and North Africa. The series collected from participating countries generally do not contain data for the most recent years mainly due to time restrictions, for example, for data quality control. The 'blended' series has these gaps infilled by an automated update procedure that relies on the daily data from synoptic messages for the same or nearby stations (within 12.5km distance and height differences less than 25m) that are transmitted in near real time over the Global Telecommunication System. The synoptic data should be replaced once the 'official' series are available from the data providers in participating countries. For more information about the underlying series used in the blending process, the quality control and homogeneity procedures, as well as comparisons with other datasets of lower temporal resolution, refer to `https://www.ecad.eu/documents/atbd.pdf` and Klein Tank et al. (2002).

More specifically in this paper we consider the blended series of snow depth from station Sonnblick, Austria, a mountaintop site in the eastern Alps (3,106m above sea level – highest observatory in the world to be operated year-round) for the period 1 November 1959 to 30 September 2016 (20,774 daily observations). The series are regularly updated, together with concentrated and enhanced efforts on data quality control and homogenization. The daily-mean temperature is given by the average of the daily-maximum and daily-minimum. The daily-mean snow depth is calculated as the average snow depth of the available values at certain times during

the day. For more information, refer to the summarized data characteristics in Table 1.

Due to its daily resolution, the ECA&D enables a variety of empirical climate studies, including detailed analyses of changes in the occurrence of extremes in relation to changes in climate variables.

## 3. Snow level and temperature modelling

In this section, we present the joint model for snow and temperature, as changes in daily temperature conditions are expected to affect not only skiing operation feasibility, but also visitors' decisions. For example, too low temperature levels can cause adverse variations in skiing demand, whereas too high temperature levels lead to snow melt, therefore, high likelihood for expensive artificial snowmaking, or shortened ski season, even ski area closure.

We model the process of the generic weather variable $W = \{S, T\}$, where $S$ denotes the snow depth and $T$ the temperature, as the sum of a predictable component $\Lambda$ and a stochastic component $\varepsilon$,

$$W_t = \Lambda_t + \varepsilon_t.$$

We discuss these two components in detail in the following.

### 3.1. Seasonality in snow and temperature

It is possible to represent the seasonal function in the following parametric form

$$\Lambda_t = \lambda_0 + \lambda_1 t + \lambda_2 \sin(2\pi t) + \lambda_3 \cos(2\pi t), \tag{1}$$

where the constant coefficients $\{\lambda_j\}$ account for deterministic regularities, i.e., seasonal fluctuations and time trend capturing long-run climate change effects. We estimate $\{\lambda_j\}$ by a non-linear regression of $W_t$ on time $t$, for $t = 1, 2, \ldots, 20{,}774$ (total number of observations), using the Matlab function `fitnlm` based on the Levenberg–Marquardt non-linear least squares algorithm (see Seber and Wild 2003). These estimates are reported alongside their standard errors and $t$-statistics in Table 2 and are statistically significantly different from zero. Not surprisingly, both the daily-mean temperature and snow depth exhibit significant regularities throughout the annual cycle with adjusted $R^2$ of 52% and 64% for the snow depth and the temperature, respectively. Moreover, the parameter estimates imply a positive (negative) trend for the temperature (snow), which can be attributed to global warming as our sample includes more than 55 years of data. From Table 2, the estimated parameter $\lambda_1$, in fact, implies that the snow level reduces by 0.49cm per year, while the temperature increases by 0.03℃ per year.

[Insert Table 2]

Alternatively, we have considered the possibility of estimating the seasonal effect in our weather variables for a particular period (e.g., January) by computing the average of the month's daily observations across all the years in the sample, bypassing any parametric functional form assumption. A visual inspection of the empirical properties of the two approaches is presented in Figures 1(a)–(d). Results from both methods are similar, with the two deseasonalized time series $\varepsilon_t$ exhibiting a significantly positive relationship (0.95 for snow, 0.96 for temperature),

with non-trivial impact on the study hereafter. For series that contain a substantial trend a more sophisticated approach might be required (e.g., see Chatfield 2004), although this is not necessary in our case.

[Insert Figure 1]

After removing $\Lambda_t$, we need to suitably model the stochastic component with the aim of generating sample trajectories of our climate variables and, subsequently, projecting the ski visitor numbers (see Section 4.1) and implementing the hedging strategies (see Section 5), which is the core of this research. To this end, in what follows, we consider, first, a (semi-)parametric bootstrap approach based on resampling of the residual series (see Section 3.2) and, second, non-parametric block bootstrap (see Section 3.3).

*3.2. An autoregressive model for the climate variables*

Consider the autoregressive (AR) model of order $q$,

$$\varepsilon_t = \phi_0 + \sum_{j=1}^{q} \phi_j \varepsilon_{t-j} + \eta_t \tag{2}$$

with $\eta_t$ independent and identically distributed random variables, and constant coefficients $\{\phi_j\}$. The parameters $\{\phi_j\}$ are estimated by maximum likelihood available through the `arima` class of Matlab and are shown in Table 3. The lag length is chosen based on the Schwarz (1978) Bayesian Information Criterion (BIC) which is smallest for orders $q = 2$ and $q = 5$ for snow and temperature, respectively. The sample Autocorrelation Function (ACF) and Partial Autocorrelation Function (PACF) plots of the filtered residuals $\{\eta_t\}$ in Figure 2 show no significant autocorrelation. More formally, we conduct a Ljung–Box Q-test at 5, 10, 15 and 20 lags, with adjusted degrees of freedom of the test statistic distribution to account for the estimated parameters. The test confirms the sample ACF and PACF results. The null hypothesis that all autocorrelations are jointly equal to zero up to the tested lag is not rejected for any of the four lags, with $p$-values ranging from 6% to 40% for the snow, and 60% to 90% for the temperature (full results available upon request). Therefore, the models capture most of the dependence (after taking care of seasonality), i.e., $\{\eta_t\}$ can be considered to be white noise.

[Insert Table 3]

[Insert Figure 2]

In order to generate sample trajectories of the stochastic component (2), we employ, by independence, standard bootstrap approach based on random resampling of the residual series $\{\eta_t\}$ corresponding to each month with replacement (Efron 1979), and feeding of the bootstrap samples into the model. In particular, random resamples $\boldsymbol{\eta}^* = (\eta_1^*, \eta_2^*, \ldots, \eta_{\tilde{n}}^*)$ are drawn from $(\eta_1, \eta_2, \ldots, \eta_n)$, where $\tilde{n}$ is the number of days of each month, and $n$ the total number of days of each month across all years in the sample, by generating $\tilde{n}$ uniformly distributed pseudorandom integers (data locations) between 1 and $n$. Due to joint modelling of the snow depth and temperature evolutions, we use common locations. By repeating several times, we obtain a collection of snow and temperature paths. Finally, as a benchmark, we fit the bivariate normal

6

distribution to snow and temperature $\eta_t$ corresponding to each month and generate sample paths using Monte Carlo simulation. The normality assumption is in line with Beyazit and Koc (2010); we formally test this in Section 3.4.

### 3.3. Block bootstrap approach to climate variables modelling

Although parametric models have been widely used to model climate variables, their pitfall is the a priori assumption of the parametric functional form of the variable to be estimated. Misspecification often occurs because restrictive assumptions can lead to misrepresentative characterization of the true data-generating process, thus resulting in inaccurate inferences. Non-parametric approaches constitute an alternative possibility as these are generally free from functional forms, hence flexible yet consistent.

To avoid breaking up the dependence in the data, we resample the data using blocks instead of individual observations[1]. By retaining the neighbouring observations together within the blocks, the dependence structure of the random variables at short lag distances is preserved. As a result, resampling blocks allows carrying this information over to the bootstrap variables. In particular, we use the moving-block stationary bootstrap introduced by Politis and Romano (1994) in which the length of block $k$, $l_k$, is generated from a geometric distribution with probability $\theta$, thus the average block length equals $1/\theta$. The $k$th block is given by $B_k = (\varepsilon_i, \varepsilon_{i+1}, \ldots, \varepsilon_{i+l_k-1})$. By randomness of the block length, the method generates random resamples which preserve the serial dependence of the original series and are also stationary. The $k$th block begins from a random index $i$ which is generated from the discrete uniform distribution on $\{1, \ldots, M\}$, where $M$ is the total number of sample dates, and random resampling with replacement is possible. As a generated block length is not limited from above, i.e., $l_k \in [1, \infty)$, and the block might begin with observation $\varepsilon_M$, the stationary bootstrap method 'wraps' the data around in a 'circle', so that $\varepsilon_1$ follows $\varepsilon_M$, and so on. The different blocks together make up a bootstrapped time series. Then, by repeating a number of times, we obtain a collection of pseudo-time series of snow and temperature. To this end, we use Kevin Sheppard's implementation of the stationary bootstrap on Matlab available freely online from `https://www.kevinsheppard.com/MFE_Toolbox`, which returns the locations of the original series, with optimal block length selected according to Politis and White (2004). As we are modelling jointly the snow depth and temperature evolutions, we use common locations.

### 3.4. Visual diagnostics and distribution backtesting

To get an idea about the fitted AR model of Section 3.2, we plot in Figures 3(a)–(b) the empirical densities of the filtered AR residuals for both snow and temperature. A closer inspection via QQ plots in Figures 3(c)–(d) indicates fat-tailed distributions, suggesting that the probability of rare events is much higher than what captured by the normal distribution. Figures 3(e)–(f) exhibit consistent time plots.

[Insert Figure 3]

---

[1]If we apply instead standard bootstrap to serially dependent observations, as is the case with weather data, the resampled series will not retain the statistical properties of the original dataset, yielding inconsistent results and statistical inference (see Ruiz and Pascual 2002).

These indications motivate us to pursue formal testing of a particular model being the true data-generating process. We assess the performance of the models by examining the distributional properties of the simulated paths. Following Diebold et al. (1998), a relevant approach is the Probability Integral Transform (PIT)[2]. More specifically, for each season commencing at $t = 1$ November $1959, 1960, \ldots, 2016$ and ending on 30 April of the same season (181 days per season), we generate the cumulative distribution forecast for each weather variable $W$. Then, at the end of every day, after the actual weather variable value $w_{t+k}$, $k = 1, \ldots, 181$, is observed, we calculate the probability of getting a value below the actual one by counting the number of generated values below that threshold; we denote this so-called transform probability by $p_{t+k}$. Under a correct distributional specification, the time series of transform probabilities (i.e., the transformed weather variable trajectories) should be distributed independently over time as a standard uniform random variable. As for a given $k$, testing the null hypothesis $H_0$: $p_{t+k} \sim i.i.d. \, \text{Unif}(0,1)$ is cumbersome due to the restricted support of the uniform distribution, we transform $p_{t+k}$ using the standard normal inverse distribution function $\Phi^{-1}(\cdot)$ and test $H_0$: $z_{t+k} = \Phi^{-1}(p_{t+k}) \sim i.i.d. \, \mathcal{N}(0,1)$ (for more details about the inverse standard cumulative normal transform of the PIT sequence, see Berkowitz 2001 based on an extension of the Rosenblatt 1952 transformation). Finally, we compute the Berkowitz (2001) statistic (likelihood ratio of normals) and the (asymptotic) probability of significance for every day $k$.

Our results (available upon request) undoubtedly favour the block bootstrap approach which yields $p$-values suggesting 70% chance, for example in the case of temperature, of no significant evidence against it, implying its ability to generate distributions that are able to replicate the historical features of the weather variables. The (semi-)parametric approach is rejected based on highly significant evidence. The test outcome is also visually reflected in Figure 4, which presents a comparison of the generated sample paths for the period 1 November to 30 April. This indicates the non-parametric method's ability to capture the seasonal mean perfectly, and adequately the 1st and 99th percentiles. (Note that the comparison against the historical percentiles is less informative as they are monthly in order to ensure a sufficiently large total number of daily observations in a month across the sample years for use in their estimation.)

[Insert Figure 4]

In light of our empirical analysis, in what follows, we focus on generating required sample trajectories of the climate variables using the block bootstrap method in lieu of parametric techniques.

## 4. Preliminary results and analysis

### 4.1. Visitor numbers

To model the ski visitor numbers, we consider the multiple regression model of Damm et al. (2014) for daily visitor numbers based on snow and temperature and several dummy variables

---

[2]Diebold et al. (1998) propose a density evaluation method which consists of computing the sequence of cumulative probability of the observed counts under the assumed forecast distribution (Probability Transform Integral). If the density fit is adequate, this sequence will be uniformly distributed.

controlling, e.g., for ski openings, particular public holidays and school breaks. The fitted regression model for the daily visitor numbers $V_t$ is

$$
\begin{aligned}
\sqrt{V_t} = {} & \alpha_0 + \alpha_1 \ln(S_t + 1) + \alpha_2 T_t + \alpha_3 \text{SkiOpening} + \alpha_4 \text{PreXmas} + \alpha_5 \text{Dec8} \\
& + \alpha_6 \text{XmasEve} + \alpha_7 \text{XmasDay} + \alpha_8 \text{SchoolHols} + \alpha_9 \text{April} \\
& + \alpha_{10} \text{Friday} + \alpha_{11} \text{Saturday} + \alpha_{12} \text{PreXmas} \times \text{Saturday} \\
& + \alpha_{13} \text{PreXmas} \times \text{Sunday} + \alpha_{14} \text{SchoolHols} \times \text{Saturday} + \epsilon_t,
\end{aligned} \tag{3}
$$

where $\epsilon_t \sim \mathcal{N}(0, \sigma^2)$, $S$ is the daily (non-negative) snow depth (cm), $T$ the daily-mean temperature (℃), dummy "SkiOpening" indicates the day(s) of the ski-opening event, "PreXmas" the period from season start to the beginning of Christmas holidays, "Dec8" the 8th December holiday, "XmasEve" the Christmas Eve, "XmasDay" the Christmas Day, "SchoolHols" the Austrian school holidays (Christmas, term break, Easter), "April" the April month (excl. Easter holidays), "Friday" the Fridays, "Saturday" the Saturdays, and "Sunday" the Sundays. The adjusted $R^2$ is 86.8%.[3]

Simulated trajectories of the climate variables using the block bootstrap approach in Section 3.3 are passed into the fitted regression model (3) in order to generate sample trajectories of daily visitor numbers. In addition, for the feasibility of skiing activities a specific minimum snow depth is required, here, 30cm. Zero visitor numbers are assumed for days with snow conditions indicating high chances for total ski area closure. Finally, we assume that our season extends from 1 November to April end (see Damm et al. 2014). From Figure 5, we can see that the simulated ski visitor numbers vary considerably during the winter season with peaks during Christmas holidays, weekends and public holidays, affecting the profitability of skiing operations. Abrupt downward movements of the visitor numbers outside the main part of the season implies that the likelihood of extreme negative outcomes is higher than what predicted by a normal model, and can be linked to lack of snow highlighting the importance of managing this type of risk.

[Insert Figure 5]

*4.2. Empirical model assessment of snow conditions and skiing operation*

Regarding the critical snow depth, a common rule in the literature (e.g., Abegg et al. 2007, Koenig and Abegg 1997, Scott et al. 2003) which is widely used nowadays for snow reliability and feasibility of skiing operations is the "100-days" rule, suggesting a snow depth of at least 30cm for at least 100 skiing days per winter season. (The rule may slightly vary, for example, Damm et al. 2014 found a threshold of 20cm to be more relevant for their analysis.)

In order to assess the reliability of snow cover, we estimate, using our simulated snow trajectories, the probability of having a specified minimum snow cover for at least 100 days

---

[3]The estimated parameters of the regression visitor model (3) are $\alpha_0 = 48.365$, $\alpha_1 = 3.8$, $\alpha_2 = -0.027$, $\alpha_3 = 11.251$, $\alpha_4 = -32.603$, $\alpha_5 = 12.522$, $\alpha_6 = -31.321$, $\alpha_7 = -21.911$, $\alpha_8 = 12.613$, $\alpha_9 = -15.103$, $\alpha_{10} = 3.856$, $\alpha_{11} = 6.574$, $\alpha_{12} = 13.1$, $\alpha_{13} = 16.076$, $\alpha_{14} = -11.438$ and $\sigma = 20$. Taking square root on the left-hand side of (3) has the advantage of not generating negative visitor numbers. In addition, it performed best in terms of $R^2$ against tested alternatives such as log-transformation. See Damm et al. (2014) for fuller details.

from 1 December until 15 April, for different initial snow levels at the beginning of the season. Figure 6 shows the results which, as expected, suggest decreasing probability the higher the minimum snow cover required; also, the lower the initial snow level, the lower the probability of achieving a given minimum snow cover. For example, a reliable snow cover of 30–50cm with at least 70% chance, consistently with the assessment of Elsasser and Messerli (2001) of snow cover reliability in 7 out of 10 winters in a (Swiss) ski area, corresponds to minimum initial snow levels of 25–40cm. Given this, in the ensuing hedging analysis, we assume an initial level of 30cm, and examine the impact of upward and downward deviations on the effectiveness of our hedging strategies. Indeed, Figure 6 shows that an initial level of 30cm ensures excess reliable snow cover of up to 60cm with 45% probability, whilst an initial level of 15cm results in just 30cm of snow cover with the same probability. An initial snow level as low as 5cm is not reliable at all, while an initial of 10cm results in a snow cover of 30cm with 11% chance.

[Insert Figure 6]

*4.3. Projection of future revenues*

We transform the projected visitor numbers from Section 4.1 into revenues by assuming a day ticket mean price for the ski season 2016/17 of $c = €29.75$ (based on 425 ski resorts, source: `http://www.skiresort.info/`); this is consistent with the projection of Damm et al. (2014) for this period for ski lift ticket prices. Figure 7 shows the cumulative percentage of total revenues over the ski season against the cumulative percentage of days. Assuming, for example, an initial level of 30cm, we find that the least-busy 50% of the days account for less than 20% of the season's total revenues. In contrast, the busiest 10% of the days account for about 30% of the revenues. Same considerations hold for the case of an initial snow level of 50cm. This is consistent with the empirical patterns observed by Hamilton et al. (2007). A lower initial level of, for example, 15cm results in least-busy 50% of the days accounting for less than 10% of the season's total revenues, whereas the busiest 10% of the days for approximately 40% of the revenues.

[Insert Figure 7]

## 5. Hedging exposure

In this section, we explore different hedging strategies that a ski resort establishment could consider in order to protect its profitability against adverse weather conditions.

As hedging positions based on weather derivatives are affected by spatial basis risk due to the difference between the weather conditions at the location of interest and the reporting station, in order to avoid unnecessary additional basis risk, the underlying of the chosen hedging instrument should be ideally directly connected to the revenues themselves, i.e., to the number of visitors at the specific resort. Given the uncertainty and discretionary nature of this type of information (i.e., not certified by some official entity), derivatives on snow and/or temperature might in a sense be easier to construct due to the fact that the information about their seasonal level is provided by independent bodies. And, indeed, as the main business activity of ski resorts

is snow sports, the risk factors affecting the firm's revenues are primarily the snow level and the temperature.

In this context, due to the observed non-linear relationship between revenue and snow level (see equation 3), viable products for hedging might be represented by options on the cumulative daily snow level over the entire season, as in Beyazit and Koc (2010). Given the direct relationship between the number of visitors and snow levels at the ski resort, typical protection against drops in profits is offered by (purchased) put option strategies; indeed, put options allow risk managers to construct portfolios with bounded revenues losses without imposing a cap on potential upside movements. We observe, though, that a potentially more effective cover could be obtained by considering periodically reset contracts on snow, possibly paired with contracts on temperature.

Thus, in the next sections, we examine these alternatives, test their effectiveness in terms of protection measured by the percentage reduction of the profits' variability, and challenge their robustness with respect to spatial basis risk. For the purpose of the analysis that follows, we denote by $p$ the premium of the option contract, $m$ the corresponding percentage markup which captures the profit margin asked by the financial institution offering the contract, and $r > 0$ the continuously compounded risk free rate of interest. As the pricing of non-standard contracts, such as weather options, is a non-trivial problem, we defer the discussion on how the premium $p$ is determined to Section 5.2.

*5.1. Hedging strategies*

Assume that the season starts at time $t_0$ and ends at $t_N$; the period $[t_0, t_N]$ is divided in $N$ equidistantly spaced sub-periods $[t_0, t_1], [t_1, t_2], \ldots, [t_{N-1}, t_N]$. Further, we assume that the hedge period coincides with the season, although allowing for forward-start hedging and/or early hedge termination is straightforward.

In order to provide a general treatment which can be adapted to several circumstances, we consider the hedging strategy as a portfolio of option contracts (cases A1–A3) or a single option (case A4); each of these financial instruments is assigned a hedge ratio representing the loss amount protected by the corresponding instrument. To this purpose, let us denote by $\boldsymbol{\vartheta}^{(A)}$ the vector of the hedge ratios characterizing the hedging strategy $(A)$. In addition, let $\chi(\boldsymbol{\vartheta}^{(A)})$ be the terminal payoff of the strategy and $\mathcal{B}(\boldsymbol{\vartheta}^{(A)})$ the corresponding (future value of the) implementation cost, i.e., the (forward) budget that the ski operator establishment needs to set aside for risk management. The functions $\chi(\boldsymbol{\vartheta}^{(A)})$ and $\mathcal{B}(\boldsymbol{\vartheta}^{(A)})$ are defined consistently with the hedge construction (see cases A1–A4 later). The resulting Profit and Loss (P&L) function of the hedged position at the end of the selected horizon is

$$\Pi^{(A)} = c \sum_{j=1}^{N} V_{t_j} + \chi(\boldsymbol{\vartheta}^{(A)}) - \mathcal{B}(\boldsymbol{\vartheta}^{(A)}).$$

The choice of the hedge ratio $\boldsymbol{\vartheta}^{(A)}$ is based on the minimum variance principle and, therefore, is the optimal solution to the minimization problem

$$\min_{\boldsymbol{\vartheta}^{(A)}} \mathrm{Var}\left(\Pi^{(A)}\right). \tag{4}$$

The P&L and its variance are computed using the simulated trajectories of the climate variables based on the block bootstrap approach in Section 3.3. Let $\tilde{\boldsymbol{\vartheta}}^{(A)}$ be the optimal solution of (4), that is, the optimal monetary value of the compensation received, and $\tilde{\Pi}$ the optimal hedge portfolio. A well-known consequence of the minimum variance principle is that $\tilde{\boldsymbol{\vartheta}}^{(A)}$ is given by the coefficient of regressing the cash flows on the option net payoff; therefore, it is determined by the covariance between the cash flows and the option net payoff, which is the key to immunization against basis risk. The hedging effectiveness is then measured by the percentage variance reduction

$$\mathcal{H} = 100 \left( 1 - \frac{\text{Var}\left(\tilde{\Pi}\right)}{\text{Var}\left(c \sum_{j=1}^{N} V_{t_j}\right)} \right) \%. \tag{5}$$

For the current analysis, the following are the alternative strategies of interest.

(A1) *Strategy S: put options on daily snow level.* The underpinning assumption is that the management of the ski resort can operate it smoothly when the current snow level is above a certain threshold $K_j^{(S)}$, referred to as the strike level, during the whole or part of the season. In this case, the hedging strategy is formed by a basket of put options on the snow level, with each contract expiring at $t_j$ for $j = 1, \ldots, N$, so that

$$\chi(\vartheta^{(S)}) = \vartheta^{(S)} \sum_{j=1}^{N} \left( K_j^{(S)} - S_{t_j} \right)^+,$$

where $x^+ = \max(x, 0)$.

The financial institution offering the contract expiring at $t_j$ adds onto the premium $p_j$ a markup $m$ in order to cover the costs of doing business and create a profit, thus the actual price charged for such a contract is $p_j(1 + m)$. Therefore, in this particular case, the implementation cost is $\vartheta^{(S)}(1 + m^{(S)}) \sum_{j=1}^{N} p_j^{(S)}$, with $m$ taking a positive or negative value consistently with the sign of $\vartheta$. The future value of the strategy is

$$\mathcal{B}(\vartheta^{(S)}) = \vartheta^{(S)}(1 + m^{(S)}) \sum_{j=1}^{N} p_j^{(S)} e^{r(t_j - t_0)}.$$

For convenience, we may hold the strikes fixed across the expiry dates $t_j$. For the details on the computation of $p_j$, we refer to Section 5.2.

(A2) *Strategy $(S, T)$: put options on daily snow and temperature levels.* As pointed out in Damm et al. (2014), for example, snow reliability of ski areas depends on the level of temperature. Indeed, as reported in Abegg et al. (2007), under a +1°C scenario only 75% of the ski areas are still snow-reliable, while this percentage drops to 61% and 30% under a +2°C and a +4°C scenario, respectively. We note, though, that too low temperatures could make skiing uncomfortable. Thus, in order to financially protect the ski resort from reduction in the number of visitors due to either too cold climate or too high temperatures that the snow begins to melt, we augment the original strategy $S$ with a strangle on temperature to achieve overall daily protection of the ski resort against both snow and

temperature exposures throughout the season (or part of it). The strangle comprises one call and one put option on temperature, with the same maturity, but different strikes $K_j^{(U,T)}$, $K_j^{(L,T)}$ for the call and put, respectively, with $K_j^{(U,T)} > K_j^{(L,T)}$. The resulting payoff of the full strategy is

$$\chi(\boldsymbol{\vartheta}^{(S,T)}) = \vartheta^{(S)} \sum_{j=1}^{N} \left( K_j^{(S)} - S_{t_j} \right)^+ + \vartheta^{(T)} \sum_{j=1}^{N} \left( \left( K_j^{(L,T)} - T_{t_j} \right)^+ + \left( T_{t_j} - K_j^{(U,T)} \right)^+ \right),$$

with future value of the implementation cost

$$\mathcal{B}(\boldsymbol{\vartheta}^{(S,T)}) = \vartheta^{(S)}(1 + m^{(S)}) \sum_{j=1}^{N} p_j^{(S)} e^{r(t_j - t_0)} + \vartheta^{(T)}(1 + m^{(T)}) \sum_{j=1}^{N} \left( p_j^{(L,T)} + p_j^{(U,T)} \right) e^{r(t_j - t_0)}.$$

For convenience, we may hold the strikes fixed across $j$.

(A3) *Strategy R: put options on monthly revenues.* In this case, we consider as the relevant underlying variable the number of visitors; the strike for the options is based on the average monthly historical revenue for the season (November, December, ..., April). Therefore, the hedge is given by a portfolio of options with terminal payoff

$$\chi(\vartheta^{(R)}) = \vartheta^{(R)} c \sum_{j=1}^{N} \left( K_j^{(R)} - V_{t_j} \right)^+ ,$$

floating strike

$$K_j^{(R)} = \frac{\sum_{k=1}^{N_j} V_{t_k}}{N_j},$$

and $N_j$ denoting the actual number of days in each month of the season. Consequently, the future cost is

$$\mathcal{B}(\vartheta^{(R)}) = \vartheta^{(R)}(1 + m^{(R)}) \sum_{j=1}^{N} p_j^{(R)} e^{r(t_j - t_0)}.$$

We note that in this strategy the relevant strike price changes every month along the hedge horizon to reflect the corresponding monthly historical average number of visitors to the resort. This differs from the previous two hedging strategies in which the strike was fixed at inception and kept constant to the end of the hedging period, although amending these to a non-constant strike, if required, would be straightforward.

(A4) *Strategy CS: put options on cumulative daily snow level as at the season end.* This strategy is based on the cumulative daily snow level at the time the position is closed, as considered in Beyazit and Koc (2010). Therefore, the hedge is formed by only one contract, and the terminal payoff is

$$\chi(\vartheta^{(CS)}) = \left( K^{(CS)} - \sum_{j=1}^{N} S_{t_j} \right)^+ ,$$

with future value of implementation cost

$$\mathcal{B}(\vartheta^{(CS)}) = \vartheta^{(CS)}(1 + m^{(CS)})p^{(CS)}e^{r(t_N - t_0)}.$$

This strategy represents the benchmark against which the other strategies are tested in terms of hedging effectiveness.

## 5.2. Option value

The identification of the optimal hedge ratio by solving the optimization problem (4) depends on the implementation cost of the hedging strategy, $\mathcal{B}$, and therefore the price $p$ of the contracts used to set up the hedge.

The problem of determining a 'fair', market-consistent price for weather derivative instruments, though, is not trivial. Indeed, standard approaches to arbitrage-free pricing (e.g., Black and Scholes 1973) are questionable in this case as, in general, it is not possible to construct a portfolio of 'tradeable' securities that replicates the payoff in question. We notice, however, that under the assumptions of a continuous-time capital asset pricing model with constant investment opportunity set, if revenues are uncorrelated with the market, then the risk can be considered as diversifiable and not be priced (see Merton 1976 and references therein). This implies that option pricing can be legitimately carried out under the physical probability measure.

For the purpose of verifying the above stated assumption, we construct an index of simulated daily returns for a hypothetical ski resort establishment using the simulated visitor numbers – specifically, we use $10,000$ daily return samples for a year. Then, we match these values to corresponding S&P 500 daily (bootstrapped) returns (see also Chance et al. 2008, for a similar application in the movie industry). A comparison of the market index returns to the daily returns of the ski establishment shows no significant correlation in bivariate Granger-causality tests, as well as regressions including contemporaneous values, at reasonable lags (up to 20). The results are confirmed when the analysis is repeated using Thomson Reuters Datastream stock indices, i.e., world, regional (for our example, Austria) and sectoral (Austria travel & leisure in our case); these are capitalization-weighted stock indices covering a minimum of 75% of the total market value.

As a result of the above, we obtain the premium for an option expiring at time $t_j$ with generic exercise price $K$ and terminal payoff $P(t_j, K)$ directly under the 'real-world' probability as

$$p_j = E_{t_0}\left(e^{-r(t_j - t_0)}P(t_j, K)\right), \tag{6}$$

where $E_{t_0}$ denotes the conditional expectation with respect to the information available at time $t_0$. We estimate (6) using the simulated values of the weather variables (cases A1, A2, A4) or visitor numbers (case A3). Given the short life of the options and the currently low interest rates, we set $r = 0$.

## 5.3. Results

The numerical analysis is organized as follows. Using $10,000$ daily sample trajectories, we solve the optimization problem (4) in correspondence of different levels of the strike prices for each strategy considered in Section 5.1 and for different initial snow levels. Specifically,

we vary the strikes $K^{(S)}$, $K^{(R)}$ and $K^{(CS)}$ in strategies $S$, $(S,T)$, $R$ and $CS$ respectively; however, we keep $K^{(L,T)}, K^{(U,T)}$ for the temperature strangle in strategy $(S,T)$ fixed at –6℃ and +4℃ respectively. This choice is based on the quantiles of the historical distribution of temperature at the resort (see, for example, Figure 4 and some common recommendation from a specialized source such as http://www.snow-forecast.com/). We note, though, that the simulation results are relatively insensitive to the chosen range for $K^{(L,T)}, K^{(U,T)}$ (more results available upon request).

As $K^{(S)}$, $K^{(R)}$ and $K^{(CS)}$ are the strikes of put options, higher values of these quantities correspond to higher option premiums, hence higher implementation costs. Thus, for comparison purposes, we report results in terms of the budget $\mathcal{B}$, also with the aim of gaining insight into the tradeoff between the hedge cover and its cost.

Results are summarized in Figures 8 and 9, in which we plot respectively the resulting optimal hedge ratios and the corresponding hedging effectiveness – as measured by the index $\mathcal{H}$ defined in equation (5) – for both different levels of the budget $\mathcal{B}$ and the initial snow level $S_0$.

[Insert Figure 8]

In details, each column of Figure 8 illustrates the optimal hedge ratios $\tilde{\vartheta}$ in correspondence of different initial level of snow $S_0$; each row, instead, classifies the optimal hedge ratios based on the originating strategy. We consider first strategies $S$, $R$ and $CS$ (rows 1, 3 and 4). The corresponding hedge ratios are all positive, consistently with the intuition of a purchased put option hedge, and decreasing as the budget level (i.e., the cost of the strategy) increases. As mentioned earlier, higher budget levels correspond to higher strike prices of the put options forming each strategy; this means that these put options move progressively more and more in the money; this implies that the payoff, and therefore the level of protection, offered by these contracts increases, as does the probability of exercise. Consequently, a smaller multiplier is required to achieve an optimal level of insurance against adverse weather movements. For these strategies, we also observe that, ceteris paribus, the optimal hedge ratios decrease as the initial level of snow increases. This reduction in the optimal hedge ratio reflects the lower probability that the put options will be exercised, due to more favourable operational conditions for the ski resort; this effect also allows to keep the cost of implementation of the strategy under control.

The second row of Figure 8 reports the optimal hedge ratios of strategy $(S,T)$; for each plot, $\tilde{\vartheta}^{(S)}$ can be read on the $y$-left-hand-axis, whilst $\tilde{\vartheta}^{(T)}$ on the $y$-right-hand-axis. In the first place, we notice that strategy $(S,T)$ entails a long position in the snow put options – similarly to strategies $S$ and $CS$ – and a short position in the temperature-based strangle. This reflects the inverse relationship between temperature and snow, and, therefore, the number of visitors at the resort and the corresponding revenues. Secondly, we note the significant difference in terms of scale between the two hedge ratios. Indeed, the (purchased) put option on snow takes a larger position in the hedging portfolio compared to the (written) strangle. Further, both $\tilde{\vartheta}^{(S)}$ and $\tilde{\vartheta}^{(T)}$ (in absolute terms) are decreasing functions of the budget $\mathcal{B}$; bearing in mind that $K^{(L,T)}, K^{(U,T)}$ are kept fixed in this analysis, the argument for $\tilde{\vartheta}^{(S)}$ is similar to what described earlier for the other strategies. This, though, implies a 'substitution' effect as $\mathcal{B}$ increases: due to increasing strikes of the snow options, the weight of the protection is shifted more and more

15

on the snow component, with consequent reduction of the amount invested in the temperature strangle.

The optimal hedge ratios $\tilde{\vartheta}^{(S)}, \tilde{\vartheta}^{(T)}$ (in absolute terms) are also decreasing functions of the initial level of snow. In case of a low level $S_0$, as already observed, the largest fraction of the hedging portfolio is represented by the (purchased) put option on snow. The (written) strangle on temperature, though, provides a useful 'top-up' which reflects the high sensitivity of the revenues to temperature movements outside the selected range and, therefore, their impact on skiing conditions. As $S_0$ increases, revenues are less exposed to these changes and consequently less protection is required. We note that, although $\tilde{\vartheta}^{(T)}$ is relatively small (in absolute value) for large $S_0$, its size reflects the residual temperature risk: on the one hand, it is conceivable to assume that higher initial levels $S_0$ are mainly related to lower temperature; the lower the temperature, the more uncomfortable skiing becomes, and as a consequence the more the put option segment of the strangle would move in the money, providing a larger portion of the hedging cover. On the other hand, copious snowfalls could also be associated with uncharacteristically high temperature levels; in such situations, though, the risk of avalanches could be high with negative repercussions on the revenues of the ski resort due to (partial) closures for related safety operations. Indeed, avalanches represent a significant fatal risk for ski tourers (see, for example, Plank 2016), the perception of which can also influence travel decisions (see Eitzinger and Wiedemann 2007, for example) and, consequently, the profitability of the ski operators. The call segment of the strangle would, in such circumstances, provide a useful floor to revenues losses.

[Insert Figure 9]

In terms of effectiveness, as shown in Figure 9, strategy $R$ provides the maximal reduction in the variance of the P&L of the position (note the different scale on the $y$-axis). This is consistent with the fact that the underlying (i.e., the visitor numbers) of the hedging put option matches the underlying of the position requiring the hedge; basis risk effects in this case are, indeed, at the minimum level. Also, consistently with intuition, strategy $CS$ based on cumulative snow level at the season end is the one performing worst amongst all considered in this analysis, especially for high initial levels of the snow $S_0$. The more flexible contracts $S$ and $(S, T)$ offer, indeed, a better control of the P&L variance thanks to the periodic reset they offer. We notice the similar performance of these two strategies, especially for a low initial snow level such as 15cm: both strategies offer up to 89% variance reduction with a similar cost of 9 million, with strategy $(S, T)$ being less expensive. For higher $S_0$ levels, the percentage variance reduction is still very similar for the two strategies, with strategy $(S, T)$ performing slightly better (for $S_0 = 50$cm, $\mathcal{H}^{(S)} = 83.17\%$ and $\mathcal{H}^{(S,T)} = 83.27\%$), while also managing to offer up to 6.85% reduction in the implementation cost; this is due to the more comprehensive cover offered by strategy $(S, T)$ which exploits the interplay between the two components as explained earlier.

The findings discussed earlier are also reflected in the implementation cost of each strategy per fixed level of the index $\mathcal{H}$. As a matter of fact, the $\mathcal{H}$ curves shown in Figure 9 are concave functions of the budget $\mathcal{B}$, with the exception of strategy $R$ whose $\mathcal{H}$ curve is – along the interval considered in this study – increasing in the level of $\mathcal{B}$. It is therefore possible to identify an

optimal value of the (optimal) hedge ratios across all budget levels and a corresponding optimal efficiency level $\mathcal{H}^*$: for the considered interval of $\mathcal{B}$, increasing the budget – and therefore the level of protection – in the case of strategies $S$, $(S, T)$ and $CS$ does not necessarily always translate in a more effective hedging of the firm's profitability.

We conclude this section with a robustness check of the results obtained above with respect to spatial basis risk due to the difference between the reference weather index to which the options forming the hedging portfolios are linked and the actual weather conditions experienced at the location of interest. Indeed, as mentioned in Section 2, our weather data refer to the Sonnblick station (Austria), whilst the parameters of the model for the number of visitors discussed in Section 4.1 refer to a study site in Styria (Austria) – see Damm et al. (2014) for full details – which is located about 95km away from the weather station. We note that such differences in weather conditions might also be due to the presence or not of artificial snow in the resort under analysis.

To this purpose, we run a sensitivity analysis by stressing the regression parameters $(\alpha_1, \alpha_2) = (3.8, -0.027)$ in equation (3) which control the dependence between the number of visitors, and therefore the revenues, and the level of snow and temperature, and determine the corresponding optimal hedge ratios and effectiveness. Specifically, we consider the cases in which both parameters are stressed by adding/subtracting multiples of their standard errors (see Damm et al. 2014), $(s_1, s_2) = (0.183, 0.005)$. Thus, we generate four alternative scenarios: $\mathcal{S}_1 = (\alpha_1 - 3s_1, \alpha_2 - 3s_2)$, $\mathcal{S}_2 = (\alpha_1 + 3s_1, \alpha_2 - 3s_2)$, $\mathcal{S}_3 = (\alpha_1 - 3s_1, \alpha_2 + 3s_2)$, $\mathcal{S}_4 = (\alpha_1 + 3s_1, \alpha_2 + 3s_2)$. We note that $\mathcal{S}_1$ and $\mathcal{S}_4$ can be interpreted, respectively, as scenarios of lower/higher 'volatility' of the visitor numbers with respect to the weather indices of relevance, and therefore as scenarios of minimum/maximum spatial basis risk.

The behaviour of the hedge ratios $\tilde{\vartheta}^{(A)}$ and the corresponding effectiveness $\mathcal{H}$ with respect to the budget level $\tilde{\mathcal{B}}^{(A)}$ is qualitatively the same as the ones of the reference case shown in Figures 8 and 9. Consistently with intuition, the hedging portfolio requires a larger position in the hedging instruments in presence of higher level of basis risk and, consequently, it becomes more expensive to maintain. Note that in the interest of readability, we do not report the actual values $\tilde{\vartheta}^{(A)}$ and $\mathcal{H}$ for each strategy in each stress scenario (complete results available upon request), but focus, instead, on the comparison of the optimal effectiveness levels of the strategies under each scenario, which we label as $\mathcal{H}_{\mathcal{S}_i}$, $i = 1, \ldots, 4$, with the one of the reference case. Results are summarized in Figure 10 and Table 4.

[Insert Figure 10]

Starting with Figure 10, the height of each bar represents the optimal effectiveness $\mathcal{H}^*$ of the reference case as identified in Figure 9; the error bars indicate the range between the largest and smallest values of $\mathcal{H}_{\mathcal{S}_i}^*$ across all the stress scenarios. We observe the following points: the largest optimal value of the hedge effectiveness is generated for all strategies by scenario $\mathcal{S}_4$, that is, $\mathcal{H}_{\mathcal{S}_4}^*$, corresponding to the case of largest possible spatial basis risk with respect to the reference case; the smallest optimal hedge effectiveness originates, instead, from scenario $\mathcal{S}_1$, that is, $\mathcal{H}_{\mathcal{S}_1}^*$, which identifies a situation with lowest level of basis risk.

Overall, the variations as indicated by the error bars are relatively small, particularly for strategy $R$; strategy $CS$, on the other hand, seems the most affected. This suggests that

the minimum variance principle, on which the construction of the hedge is based, performs successfully in keeping the basis risk at a minimum level, so that even a sub-optimal hedging ratio (with respect to the actual weather conditions at the location of interest) is relatively satisfactory in offering an effective risk cover. The robust performance is supported by the non-linearity of the contracts chosen for the purpose, and their design – consistently with our previous findings. Thus, these observations suggest that for hedging principles robust with respect to basis risk, such as the minimum variance one, the choice of the weather station is less critical in managing the spatial basis risk in the case of weather derivatives. This is also consistent with the findings of Manfredo and Richards (2009).

These results are also confirmed with respect to the tradeoff between efficiency levels and cost of the hedge, i.e., the budget level $\mathcal{B}$. In order to better quantify this aspect, we argue as follows. Recall that the reference case is characterized by an optimal hedge effectiveness $\mathcal{H}^*$ which is achieved with an implementation cost $\mathcal{B}^*$; similarly, the stress scenarios $\mathcal{S}_i$, $i = 1, \ldots, 4$, are associated with an optimal effectiveness $\mathcal{H}^*_{\mathcal{S}_i}$ with cost $\mathcal{B}^*_{\mathcal{S}_i}$. The tradeoff between efficiency and cost can then be quantified by the multiplier

$$\mathrm{M}_{\mathcal{S}_i} = \frac{\mathcal{H}^*_{\mathcal{S}_i} \mathcal{B}^*_{\mathcal{S}_i}}{\mathcal{H}^* \mathcal{B}^*}, \quad i = 1, \ldots, 4, \tag{7}$$

of the budget that is requested in scenario $\mathcal{S}_i$ to achieve a particular effectiveness level compared to the reference case. If $\mathrm{M} > 1 \ (< 1)$, the hedging portfolio in the reference case is (is not) to be preferred to the one of scenario $\mathcal{S}_i$. The multipliers of each strategy are reported in Table 4 for all stress scenarios and initial snow levels considered in this study; the numbers confirm the relative robust performance of the proposed hedges with respect to basis risk.

[Insert Table 4]

## 6. Conclusions

We propose a methodology for the identification of effective hedging strategies for ski tourism operators based on weather derivatives, such as snow and temperature options. The framework consists of a non-parametric approach based on block bootstrap for the modelling of the evolution of these variables, a regression model for the number of visitors at the resort, which determines its revenues, a valuation method for the derivatives, and the minimum variance principle for the computation of the relevant hedge ratios. Our simulation study shows the superior performance of hedging strategies based on portfolios with periodic reset of snow options, and combination of snow and temperature options.

Our analysis focuses on natural snow conditions, and therefore does not include artificial snow. The motivation behind this choice is to focus on the role of weather derivatives as tools for stabilizing business profitability and facilitating the implementation and maintenance of adaptation strategies such as snowmaking, whose economic profitability is threatened, too, by climate change (see Damm et al. 2014).

The results reported in this paper refer to the case of one single resort; the analysis could be extended to the case of ski conglomerates with multiple properties on the line of the work of Tang and Jang (2011), but we leave this to future research.

18

## Acknowledgements

## References

Abegg, B., Agrawala, S., Crick, F., de Montfalcon, A., 2007. Climate change impacts and adaptation in winter tourism. In: Agrawala, S. (Ed.), Climate Change in the European Alps. Adapting Winter Tourism and Natural Hazards Management. OECD, pp. 25–60.

ANTO, January 2016. Factsheet Tourism in Austria 2015. Austrian National Tourist Office. URL https://newsroom-en.austriatourism.com/files/2016g_factsheet-tourism-in-austria-2015-english-02-03-2016.pdf

Baggio, R., Sainaghi, R., 2016. Mapping time series into networks as a tool to assess the complex dynamics of tourism systems. Tourism Management 54, 23–33.

Bank, M., Wiesner, R., 2011. Determinants of weather derivatives usage in the austrian winter tourism industry. Tourism Management 32 (1), 62–68.

Berkowitz, J., 2001. Testing density forecasts, with applications to risk management. Journal of Business & Economic Statistics 19 (4), 465–474.

Beyazit, M. F., Koc, E., 2010. An analysis of snow options for ski resort establishments. Tourism Management 31 (5), 676–683.

Black, F., Scholes, M., 1973. The pricing of options and corporate liabilities. Journal of Political Economy 81 (3), 637–654.

Broll, U., Chow, K. W., Wong, K. P., 2001. Hedging and nonlinear risk exposure. Oxford Economic Papers 53 (2), 281–296.

Cavallaro, F., Ciari, F., Nocera, S., Prettenthaler, F., Scuttari, A., 2017. The impacts of climate change on tourist mobility in mountain areas. Journal of Sustainable Tourism 25 (8), 1063–1083.

Chance, D. M., Hillebrand, E., Hilliard, J. E., 2008. Pricing an option on revenue from an innovation: An application to movie box office revenue. Management Science 54 (5), 1015–1028.

Chatfield, C., 2004. The Analysis of Time Series: An Introduction. Texts in Statistical Science. Chapman & Hall/CRC, Boca Raton.

Damm, A., Greuell, W., Landgren, O., Prettenthaler, F., 2017. Impacts of +2°C global warming on winter tourism demand in Europe. Climate Services 7, 31–46.

Damm, A., Köberl, J., Prettenthaler, F., 2014. Does artificial snow production pay under future climate conditions? – A case study for a vulnerable ski area in Austria. Tourism Management 43, 8–21.

Dawson, J., Scott, D., 2013. Managing for climate change in the alpine ski sector. Tourism Management 35, 244–254.

Diebold, F. X., Gunther, T. A., Tay, A. S., 1998. Evaluating density forecasts with applications to financial risk management. International Economic Review 39 (4), 863–883.

Đorđević, B. S., 2018. Hedging by using weather derivatives in winter ski tourism. Economics of Agriculture 65 (1), 125–142.

Efron, B., 1979. Bootstrap methods: Another look at the jackknife. The Annals of Statistics 7 (1), 1–26.

Eitzinger, C., Wiedemann, P., 2007. Risk perceptions in the alpine tourist destination Tyrol–An exploratory analysis of residents' views. Tourism Management 28 (3), 911–916.

Elsasser, H., Messerli, P., 2001. The vulnerability of the snow industry in the Swiss Alps. Mountain Research and Development 21 (4), 335–339.

Falk, M., Hagsten, E., 2016. Importance of early snowfall for swedish ski resorts: Evidence based on monthly data. Tourism Management 53, 61–73.

Hamilton, L. C., Brown, C., Keim, B. D., 12 2007. Ski areas, weather and climate: time series models for New England case studies. International Journal of Climatology 27 (15), 2113–2124.

Klein Tank, A. M. G., Wijngaard, J. B., Können, G. P., Böhm, R., Demarée, G., Gocheva, A., Mileta, M., Pashiardis, S., Hejkrlik, L., Kern-Hansen, C., Heino, R., Bessemoulin, P., Müller-Westermeier, G., Tzanakou, M., Szalai, S., Pálsdóttir, T., Fitzgerald, D., Rubin, S., Capaldo, M., Maugeri, M., Leitass, A., Bukantis, A., Aberfeld, R., van Engelen, A. F. V., Forland, E., Mietus, M., Coelho, F., Mares, C., Razuvaev, V., Nieplova, E., Cegnar, T., Antonio López, J., Dahlström, B., Moberg, A., Kirchhofer, W., Ceylan, A., Pachaliuk, O., Alexander, L. V., Petrovic, P., 2002. Daily dataset of 20th-century surface air temperature and precipitation series for the European Climate Assessment. International Journal of Climatology 22 (12), 1441–1453.

Koenig, U., Abegg, B., 1997. Impacts of climate change on winter tourism in the Swiss Alps. Journal of Sustainable Tourism 5 (1), 46–58.

Manfredo, M. R., Richards, T. J., 2009. Hedging with weather derivatives: a role for options in reducing basis risk. Applied Financial Economics 19 (2), 87–97.

Merton, R. C., 1976. Option pricing when underlying stock returns are discontinuous. Journal of Financial Economics 3 (1), 125–144.

Plank, A., 2016. The hidden risk in user-generated content: An investigation of ski tourers' revealed risk-taking behavior on an online outdoor sports platform. Tourism Management 55, 289–296.

Politis, D. N., Romano, J. P., 1994. The stationary bootstrap. Journal of the American Statistical Association 89 (428), 1303–1313.

Politis, D. N., White, H., 2004. Automatic block-length selection for the dependent bootstrap. Econometric Reviews 23 (1), 53–70.

Rosenblatt, M., 1952. Remarks on a multivariate transformation. The Annals of Mathematical Statistics 23 (3), 470–472.

Ruiz, E., Pascual, L., 2002. Bootstrapping financial time series. Journal of Economic Surveys 16 (3), 271–300.

Schwarz, G., 1978. Estimating the dimension of a model. The Annals of Statistics 6 (2), 461–464.

Scott, D., McBoyle, G., 2006. Climate change adaptation in the ski industry. Mitigation and Adaptation Strategies for Global Change 12 (8), 1411–1431.

Scott, D., McBoyle, G., Mills, B., 2003. Climate change and the skiing industry in southern Ontario (Canada): exploring the importance of snowmaking as a technical adaptation. Climate Research 23 (2), 171–181.

Seber, G. A. F., Wild, C. J., 2003. Nonlinear Regression. Wiley-Interscience, Hoboken, NJ.

Steiger, R., Abegg, B., 2013. The sensitivity of Austrian ski areas to climate change. Tourism Planning & Development 10 (4), 480–493.

STV-FST, 2016. Swiss Tourism in Figures 2015 – Structure and Industry Data. Schweizer Tourismus–Verband.

Tang, C.-H., Jang, S., 2011. Weather risk management in ski resorts: Financial hedging and geographical diversification. International Journal of Hospitality Management 30 (2), 301–311.

Tang, C.-H., Jang, S., 2012. Hedging weather risk in nature-based tourism business: An example of ski resorts. Journal of Hospitality & Tourism Research 36 (2), 143–163.

Toeglhofer, C., Mestel, R., Prettenthaler, F., 2012. Weather value at risk: On the measurement of noncatastrophic weather risk. Weather, Climate, and Society 4 (3), 190–199.

Wolfsegger, C., Gössling, S., Scott, D., 2008. Climate change risk appraisal in the austrian ski industry. Tourism Review International 12 (1), 13–23.

WTTC, March 2017. Travel & Tourism – Economic Impact 2017, European Union LCU. World Travel & Tourism Council.
URL `https://www.wttc.org/-/media/files/reports/economic%20impact%20research/regions%202016/europelcu2016.pdf`

Wyss, R., Abegg, B., Luthe, T., 2014. Perceptions of climate change in a tourism governance context. Tourism Management Perspectives 11, 69–76.

| Data characteristics | |
|---|---|
| Station name | Sonnblick |
| Latitude (°:′:″) | +47:03:00 |
| Longitude (°:′:″) | +012:57:00 |
| Station elevation (m) | 3,106 |
| Period | 1-Nov-59–30-Sept-16 |
| Frequency of observation | Daily (20,774 observations) |
| Daily-mean temperature | Average daily-max (06–18 UT) & daily-min (18 UT–06 UT current day) |
| Daily-mean snow depth | Average available values at 00, 06, 12 and/or 18 UT |

Table 1: The table presents the summarized data characteristics. *Notes.* UT: Universal Time; Latitude: $+ (-)$ refers to North (South); Longitude: $+ (-)$ refers to East (West).

| Deterministic snow component | | | | |
|---|---|---|---|---|
| Coefficient | Estimate | Standard error | $t$-statistic | $p$-value |
| $\lambda_0$ | 273.0304 | 1.5867 | 172.0773 | 0.0000 |
| $\lambda_1$ | -0.4948 | 0.0483 | -10.2532 | 0.0000 |
| $\lambda_2$ | 10.2382 | 1.1217 | 9.1274 | 0.0000 |
| $\lambda_3$ | -167.8955 | 1.1222 | -149.6184 | 0.0000 |

| Deterministic temperature component | | | | |
|---|---|---|---|---|
| Coefficient | Estimate | Standard error | $t$-statistic | $p$-value |
| $\lambda_0$ | -6.2447 | 0.0562 | -111.1072 | 0.0000 |
| $\lambda_1$ | 0.0361 | 0.0017 | 21.1220 | 0.0000 |
| $\lambda_2$ | -7.6187 | 0.0397 | -191.7430 | 0.0000 |
| $\lambda_3$ | 0.7850 | 0.0397 | 19.7478 | 0.0000 |

Table 2: The table presents the estimates for the deterministic snow and temperature components $\Lambda_t$ (see equation 1) (number of observations = 20,774; root mean squared error = 114 – snow, 4.05 – temperature; adjusted $R^2$ = 0.521 – snow, 0.645 – temperature; $F$-statistic vs. constant model = 7.52e+03 – snow, 1.26e+04 – temperature with $p$-value = 0 – both).

| Deseasonalized snow component | | | | |
|---|---|---|---|---|
| Coefficient | Estimate | Standard error | $t$-statistic | $p$-value |
| $\phi_0$ | 0.0002 | 0.1087 | 0.0018 | 0.0000 |
| $\phi_1$ | 1.0974 | 0.0033 | 331.9910 | 0.0000 |
| $\phi_2$ | -0.1046 | 0.0033 | -32.0859 | 0.0000 |

| Deseasonalized temperature component | | | | |
|---|---|---|---|---|
| Coefficient | Estimate | Standard error | $t$-statistic | $p$-value |
| $\phi_0$ | 0.0003 | 0.0163 | 0.0193 | 0.0000 |
| $\phi_1$ | 1.0656 | 0.0055 | 193.3800 | 0.0000 |
| $\phi_2$ | -0.4423 | 0.0078 | -56.4655 | 0.0000 |
| $\phi_3$ | 0.1933 | 0.0089 | 21.6681 | 0.0000 |
| $\phi_4$ | -0.0484 | 0.0091 | -5.3197 | 0.0000 |
| $\phi_5$ | 0.0231 | 0.0064 | 3.5855 | 0.0000 |

Table 3: The table presents the estimates of the fitted AR(2) and AR(5) model, respectively, for the deseasonalized snow and temperature components $\varepsilon_t$ (see equation 2) (Bayesian information criterion = 1.6532e+05 – snow, 9.3401e+04 – temperature; Anderson–Darling test for normality $p$-value $< 0.0005$ – both). The estimates remained unaffected by the choice between parametric seasonality (see equation 1) and non-parametric estimation of the seasonal effect (see relevant discussion in Section 3.1).

| $S_0$ | Strategy | $\mathcal{S}_1$ | $\mathcal{S}_2$ | $\mathcal{S}_3$ | $\mathcal{S}_4$ |
|---|---|---|---|---|---|
| | $S$ | 0.92 | 1.07 | 0.92 | 1.12 |
| | $S,T$ | 0.92 | 1.06 | 0.93 | 1.15 |
| 15cm | $R$ | 0.96 | 1.07 | 0.96 | 1.05 |
| | $CS$ | 0.91 | 1.08 | 0.90 | 1.25 |
| | $S$ | 0.80 | 0.99 | 0.81 | 1.12 |
| | $S,T$ | 0.80 | 0.98 | 0.81 | 1.10 |
| 30cm | $R$ | 0.98 | 1.05 | 0.96 | 1.07 |
| | $CS$ | 0.82 | 1.09 | 0.85 | 1.25 |
| | $S$ | 0.92 | 1.08 | 0.87 | 1.28 |
| | $S,T$ | 0.87 | 0.97 | 0.85 | 1.21 |
| 50cm | $R$ | 0.98 | 0.96 | 0.98 | 1.04 |
| | $CS$ | 0.85 | 1.06 | 0.91 | 1.26 |

Table 4: The table presents the multipliers $\mathrm{M}_{\mathcal{S}_i}$ (see equation 7) for different initial levels of snow $S_0 = 15, 30, 50$cm, and hedging strategies in scenarios $\mathcal{S}_i$, $i = 1, \ldots, 4$, obtained by stressing the coefficient parameters of snow level and temperature in the regression model of the number of visitors (see equation 3). In details: $\mathcal{S}_1 = (\alpha_1 - 3s_1, \alpha_2 - 3s_2)$, $\mathcal{S}_2 = (\alpha_1 + 3s_1, \alpha_2 - 3s_2)$, $\mathcal{S}_3 = (\alpha_1 - 3s_1, \alpha_2 + 3s_2)$, $\mathcal{S}_4 = (\alpha_1 + 3s_1, \alpha_2 + 3s_2)$. Contract parameters: ticket price $c = €29.75$; option price markup $m^{(S)} = m^{(S,T)} = m^{(R)} = m^{(CS)} = 10\%$; $K^{(L,T)} = -6$°C, $K^{(U,T)} = +4$°C.
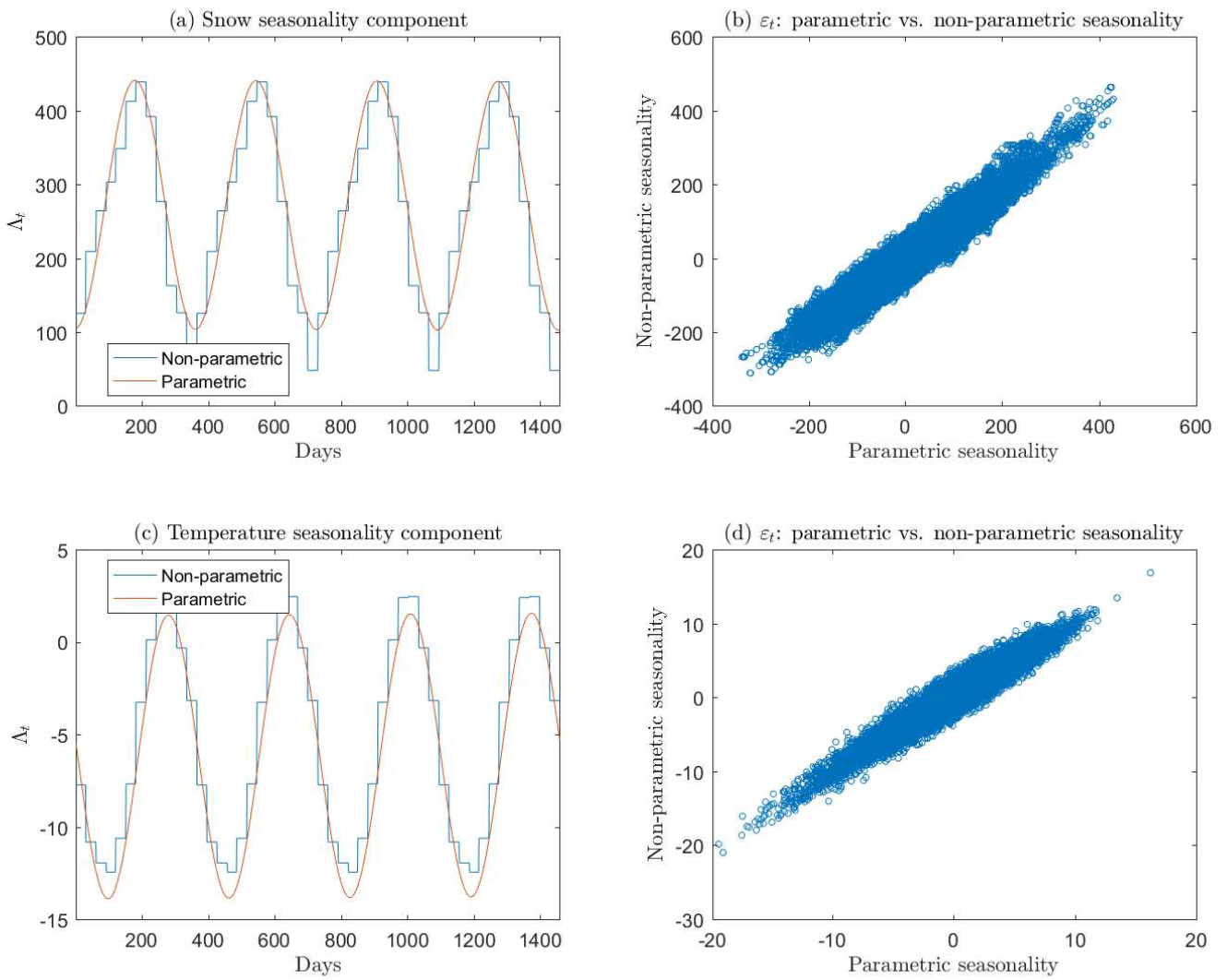
Figure 1: *Snow and temperature seasonality.* The figure presents (a), (c) the fitted deterministic seasonality component (see equation 1) versus the average snow level / temperature for each month; (b), (d) the scatterplot of deseasonalized components using parametric versus non-parametric seasonality.
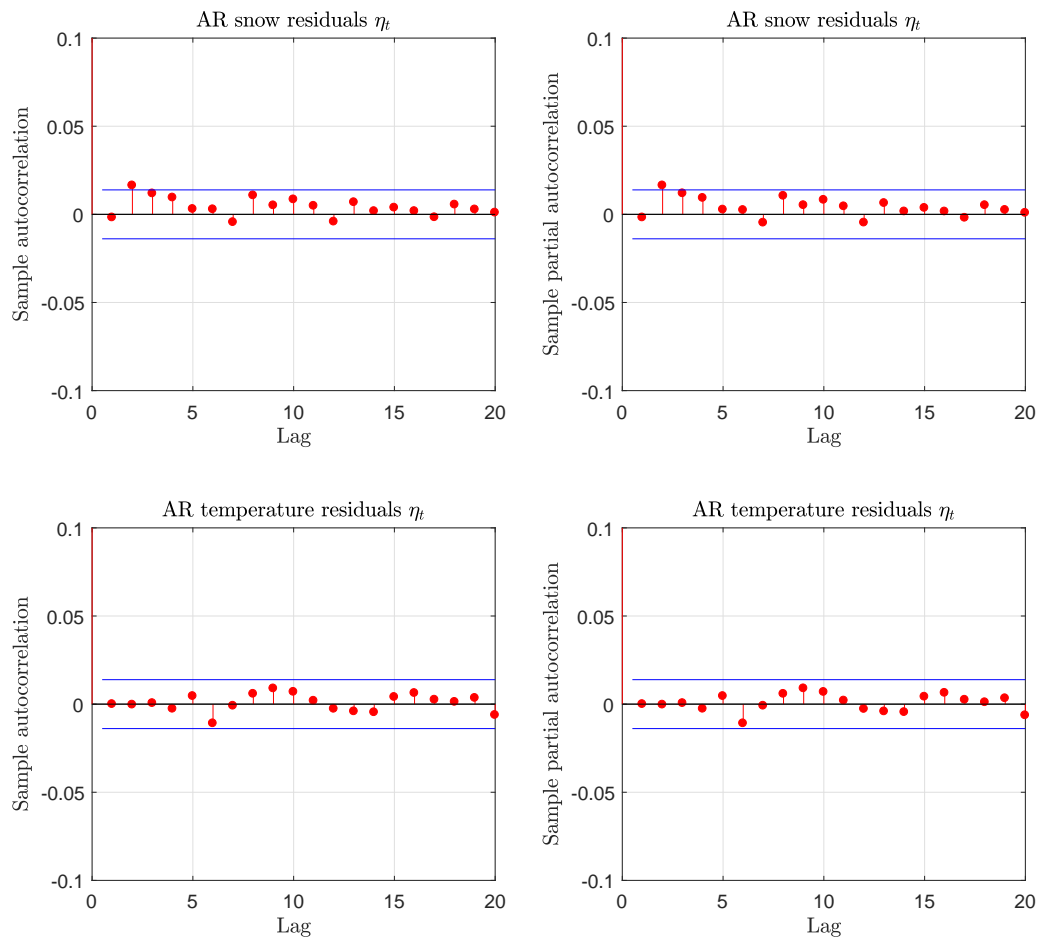
Figure 2: *AR snow and temperature residuals autocorrelations.* The figure presents the sample (partial) autocorrelation function of AR(2) snow residuals and AR(5) temperature residuals, $\eta_t$.
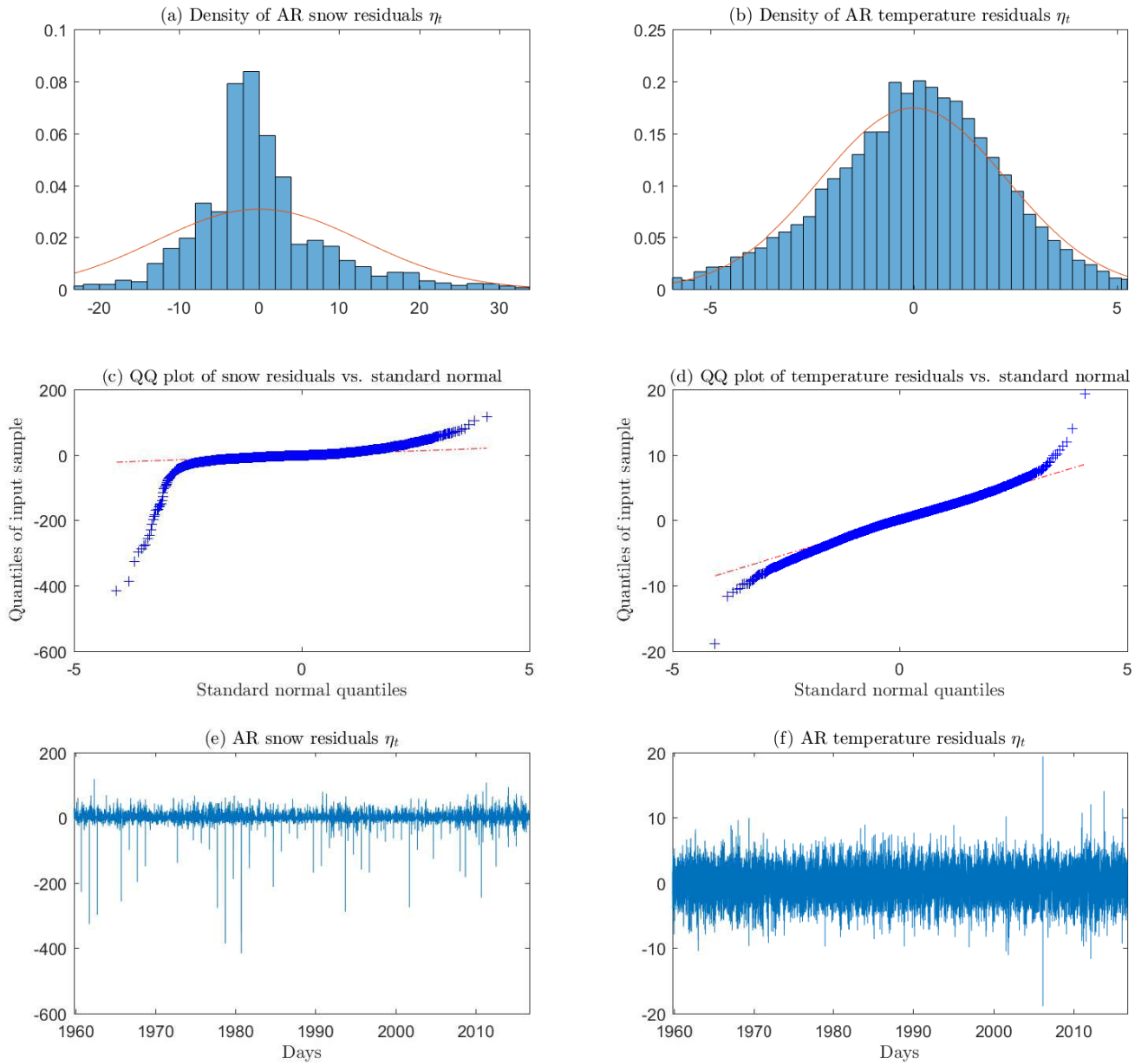
Figure 3: *Distributional characteristics of AR snow and temperature residuals.* The figure presents (a)–(b) the empirical densities of the snow and temperature residuals, $\eta_t$, after fitting, respectively, the AR(2) and AR(5) models to the deseasonalized components (see equation 2) against a normal density (indicated by the continuous plot); (c)–(d) the QQ plots of the quantiles of the residuals against the theoretical quantile values from the standard normal distribution (the plot appears linear if the distribution of the residuals is normal); (e)–(f) the time plot of the residuals for the period 1 November 1959 to 30 September 2016.
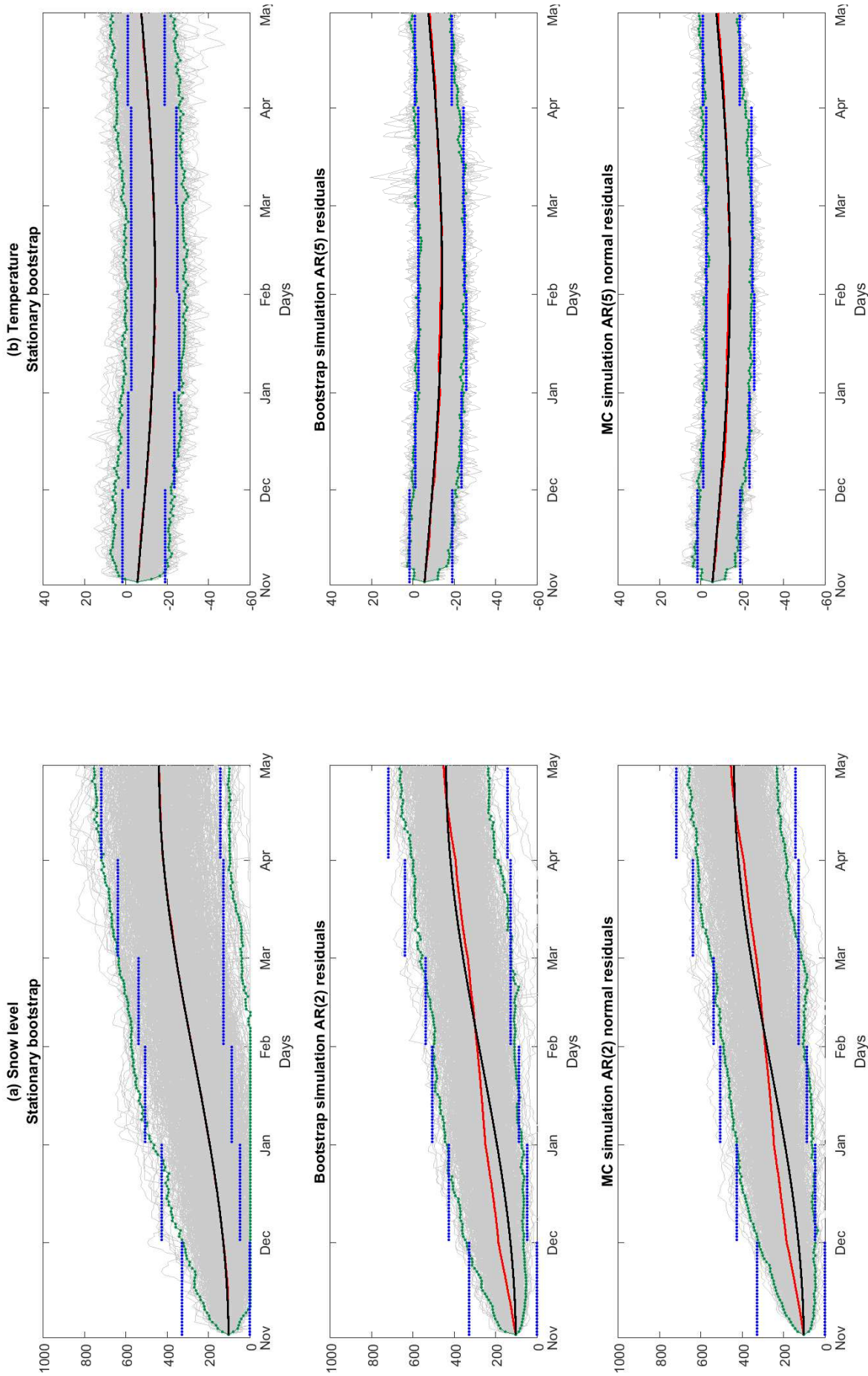
Figure 4: *Snow and temperature sample trajectories.* The figure presents snow and temperature sample trajectories for the ski season 1 November to 30 April (181 days) generated by moving-block stationary bootstrap, standard bootstrap of AR residuals, and Monte Carlo (MC) simulation of fitted normal AR residuals. In addition, it presents simulated 1st and 99th percentiles (green point lines) versus historical estimates of 1st and 99th percentiles for each month (blue flat lines), and simulated means (red solid lines) versus seasonal means (black solid lines).

28
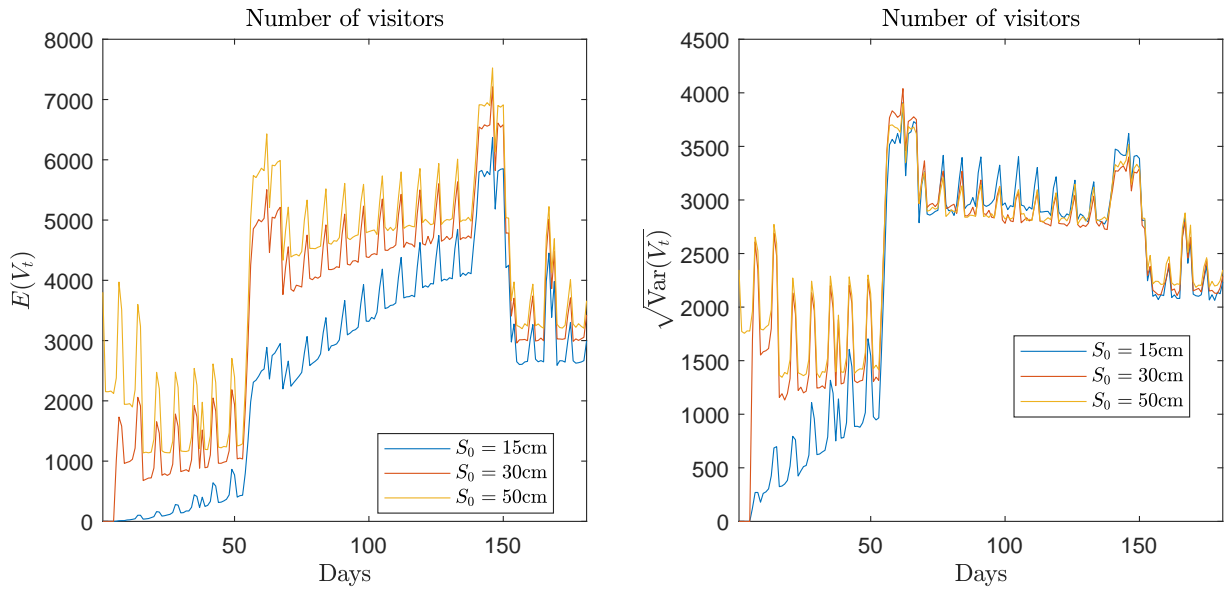
Figure 5: *Statistics of visitor numbers.* The figure presents the mean and standard deviation of the projected daily numbers of visitors for the ski season 1 November to 30 April, for different initial levels of snow $S_0 = 15, 30, 50$cm.
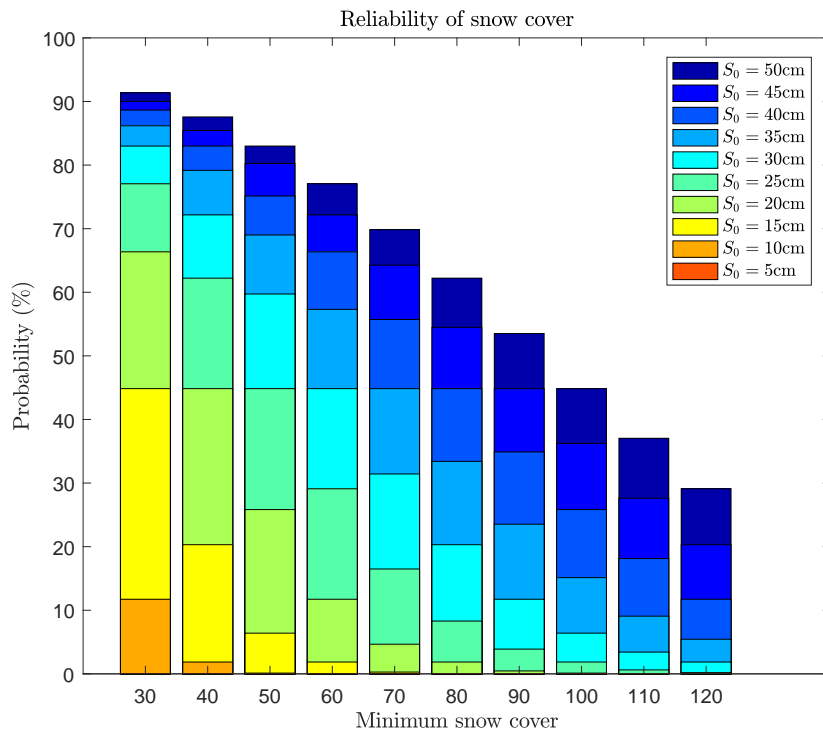


Figure 6: *Implementation of "100-days" rule for snow reliability.* The figure presents the probability estimates of having different specified minimum snow covers for at least 100 days from 1 December until 15 April, for different initial levels of snow.

(a) $S_0 = 15$cm
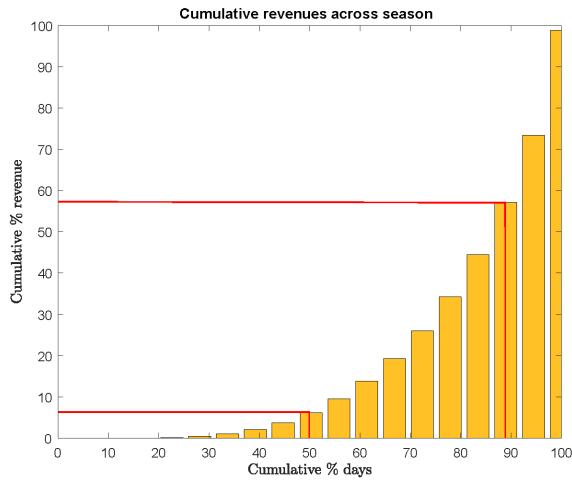
(b) $S_0 = 30$cm
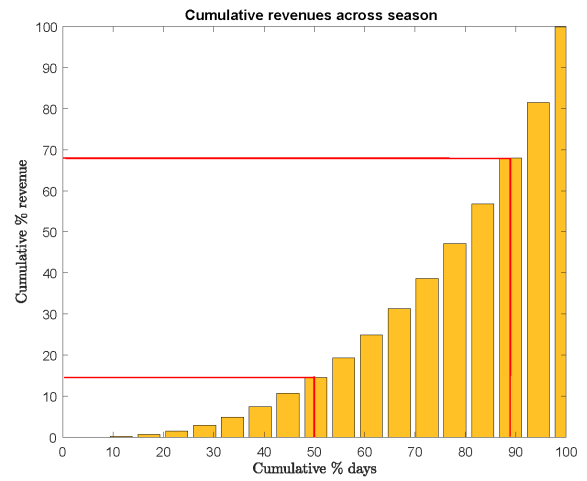


(c) $S_0 = 50$cm
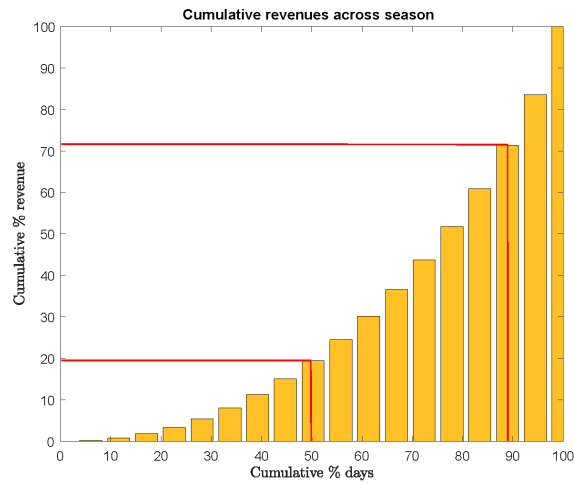


Figure 7: *Analysis of revenues over season.* The figure presents the cumulative percentage of total revenues over the ski season against the cumulative percentage of days, for different initial levels of snow $S_0 = 15, 30, 50$cm. Note that the top red solid line indicates the revenue of the busiest 10% of the days; the bottom red solid line indicates the revenue of the least-busy 50% of the days.

(a) $S_0 = 15$cm         (b) $S_0 = 30$cm         (c) $S_0 = 50$cm
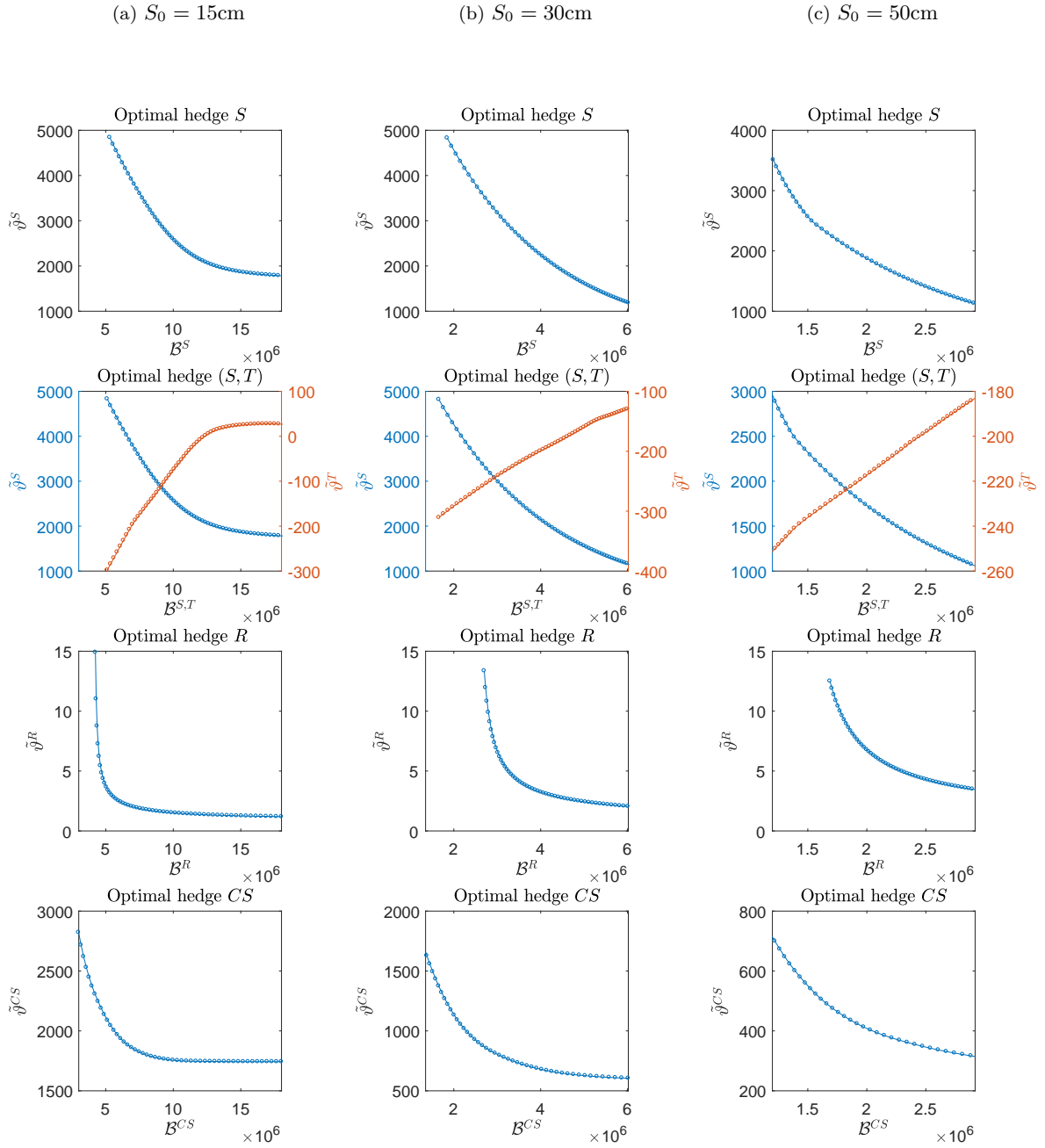
Figure 8: *Optimal hedges.* The figure summarizes the different optimal hedges, for different initial levels of snow $S_0 = 15, 30, 50$cm. Contract parameters: ticket price $c = €29.75$; option price markup $m^{(S)} = m^{(S,T)} = m^{(R)} = m^{(CS)} = 10\%$; $K^{(L,T)} = -6$°C, $K^{(U,T)} = +4$°C.

(a) $S_0 = 15$cm



(b) $S_0 = 30$cm



(c) $S_0 = 50$cm
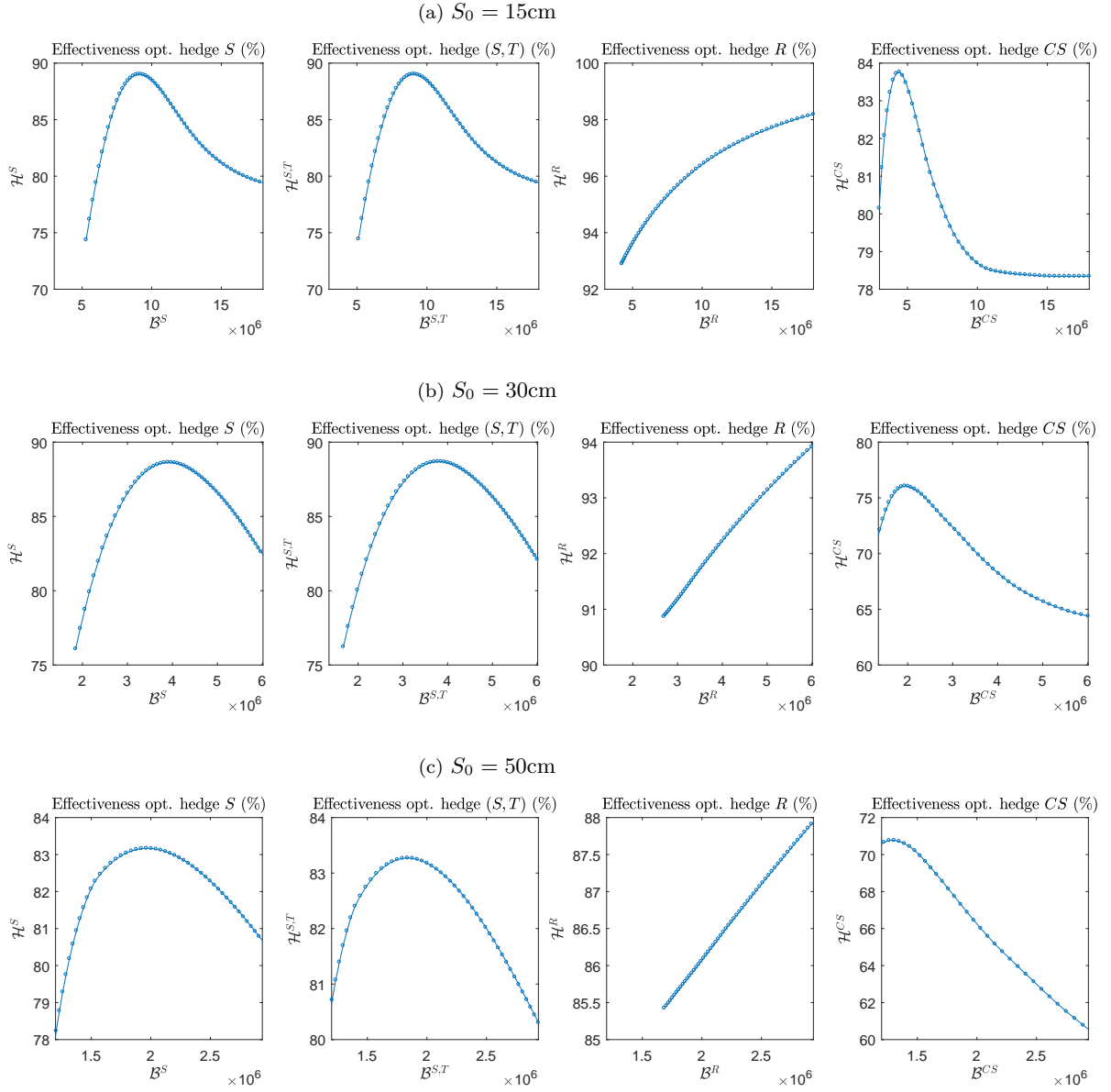


Figure 9: *Hedging effectiveness.* The figure summarizes the effectiveness of the different optimal hedges, for different initial levels of snow $S_0 = 15, 30, 50$cm. Contract parameters: ticket price $c =$ €29.75; option price markup $m^{(S)} = m^{(S,T)} = m^{(R)} = m^{(CS)} = 10\%$; $K^{(L,T)} = -6$℃, $K^{(U,T)} = +4$℃.
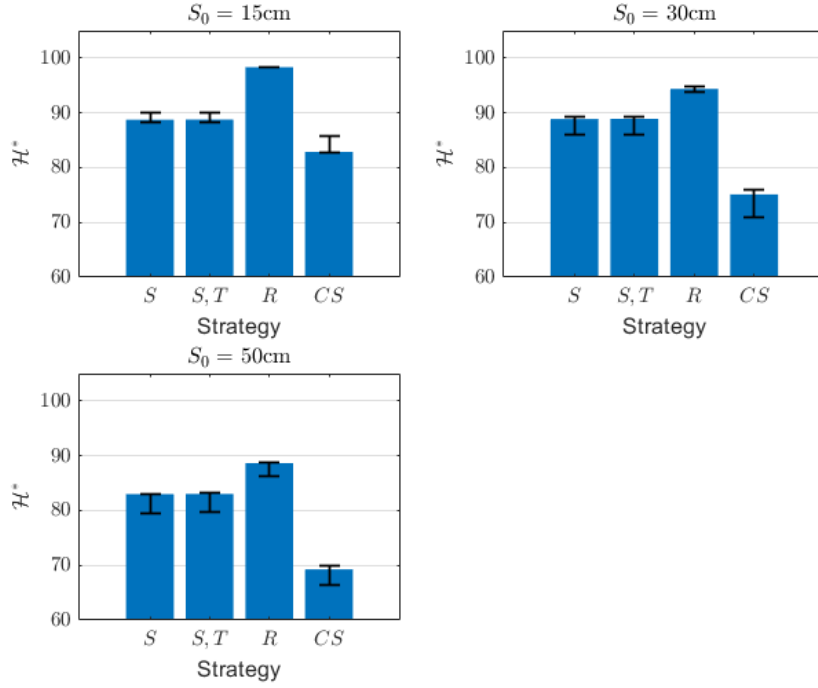
Figure 10: *Impact of spatial basis risk on hedging effectiveness.* The figures exhibit for different initial levels of snow $S_0 = 15, 30, 50$cm the optimal hedging effectiveness level $\mathcal{H}^*$ for the reference case identified in Figure 9. Error bars indicate the range between the largest and smallest optimal values of $\mathcal{H}^*_{\mathcal{S}_i}$, with $\mathcal{S}_1 = (\alpha_1 - 3s_1, \alpha_2 - 3s_2)$, $\mathcal{S}_2 = (\alpha_1 + 3s_1, \alpha_2 - 3s_2)$, $\mathcal{S}_3 = (\alpha_1 - 3s_1, \alpha_2 + 3s_2)$, $\mathcal{S}_4 = (\alpha_1 + 3s_1, \alpha_2 + 3s_2)$. Contract parameters: ticket price $c = €29.75$; option price markup $m^{(S)} = m^{(S,T)} = m^{(R)} = m^{(CS)} = 10\%$; $K^{(L,T)} = -6$℃, $K^{(U,T)} = +4$℃.